1-1-2008

Stiffness characterisation of microcantilevers based on conducting polymers

Gursel Alici
University of Wollongong, gursel@uow.edu.au

Michael J. Higgins
University of Wollongong, mhiggins@uow.edu.au

Stiffness characterisation of microcantilevers based on conducting polymers

Gursel Alici[a*], Michael J. Higgins[b]
[a]University of Wollongong, School of Mechanical, Materials and Mechatronic Engineering;
[b]University of Wollongong, Intelligent Polymer Research Institute, Australia

ABSTRACT

The object of this paper is to characterise the stiffness of microfabricated cantilevers consisting of two electroactive polymer (polypyrrole (PPy)) layers, and two gold layers with a negligible thickness and a layer of porous polyvinylidene fluoride (PVDF), which serves as a backing layer and electrolyte storage tank. This composite cantilever structure is used as polymer actuators or famously known as artificial muscles when tailored appropriately. The polymer microactuators considered in this study, which were fabricated using a laser ablation technique, could operate both in aqueous and non-aqueous media. The stiffness characterization of the microactuators is critical to assess their suitability to numerous applications including the micromanipulation of living cells, bio-analytical nanosystems, datastorage, lab-on-chip, microvalve, microswitch, microshutter, cantilever light modulators, micro-optical instrumentation, artificial muscles for micro and macro robotic sytems and similar. The stiffness measurement method followed in this study is a static deflection measurement method, using an atomic force microscope (AFM). The stiffness constants of the microactuators while they were in passive (no electrochemical activation) and active (electrochemically activated) states were measured separately, and their statistical comparison was provided. The possible error sources for the stiffness measurement method are elaborated.

Keywords: electroactive polymers, microactuators, stiffness characterisation, microfabrication, atomic force microscopy

1. INTRODUCTION

The next generation of Micro-Electro-Mechanical Systems (MEMS) and future development of Nano-Electro-Mechanical Systems (NEMS) depend on continued progress in actuator fabrication methods and the introduction of novel actuator materials. With this in mind, there is an increasing need for suitable MEMS actuation means that are robust, require low power, have small footprints and can operate in wet and dry environments. Microsized conducting polymer actuators fulfill the needs of MEMS applications and lay a foundation for future nano-scale devices. Further, compared to inorganic materials such as polysilicon, the compliant properties of the polymer actuators allow the resumption of normal operation after the actuator has been subject to significant mechanical forces, or disturbance [1]. By incorporating electroactive polymers (EAP) in MEMS, the fabrication of the actuator elements is simplified. For MEMS devices, the advantages of EAP include their larger actuation at lower voltages, insensitivity to magnetic fields, operation in air and wet media; biocompatibility and additional functionality for controlled drug release and chemical sensing applications.

Although significant attempts have been directed towards the synthesis, performance quantification, positioning improvement and applications of non-aqueous polypyrrole (PPy) conducting polymer actuators with lengths greater than 5 mm [2-5], to our knowledge there has been no reports on microsized all-solid state polymer actuators, except [1]. A primary reason for this is that the synthesis technique and structure of the dry-type actuators is not quite conducive to the use of conventional lithographic techniques for fabricating actuators < 1 mm in length.

Stiffness characterization of the microactuators is critical for assessing their ability to withstand mechanical forces, and for knowing the forces that they will apply to the external environment (e.g. when gripping an object). In this context, a comprehensive review of various methods to determine the normal stiffness, or 'stiffness constant', of micron-sized

* gursel@uow.edu.au; phone 61 2 4221-4145; fax 61 2 4221-3101.

Smart Structures, Devices, and Systems IV, edited by Said Fares Al-Sarawi,
Vijay K. Varadan, Neil Weste, Kourosh Kalantar-Zadeh, Proc. of SPIE Vol. 7268, 726806

cantilevers used in Atomic Force Microscopy (AFM) [6] highlights the possibility of adapting such methods for calibrating similar sized EAP microactuators. This idea of applying AFM-based techniques forms the basis of this study, which involves utilizing a modified approach of the reference stiffness method [8] to measure the stiffness constant of rectangular polypyrrole microactuators. This method uses the Hooke's Law to calculate the stiffness constant, k, by pushing an AFM cantilever against the polymer microactuator with a known force, F, and then measuring the resulting displacement, D, of the polymer microactuator. Due to its simple implementation, we found this method to be most amenable for our measurements in comparison to other AFM calibration techniques such as the Added Mass, Thermal Noise and Sader Methods [7-9]. Although, in principle, it is possible to use these other techniques, they were deemed less applicable due to their requirement for a direct measurement of the polymer microactuator displacement. For these calibration procedures, the latter is needed to obtain parameters such as the fundamental resonance frequency, thermal noise spectra and/or quality factor and typically requires a specially designed detection system (e.g. optical detection) for measurement of the cantilever beam displacement. For practical reasons, a detection system for the polymer microactuators was not employed in this study, while alternative attempts to use the AFM optical detection system by positioning the polymer microactuators in the AFM was unsuccessful. This was due to two reasons (i) a lack of reflectivity from the surface of the polymer microactuator to generate a sufficient signal in the photodiode, and (ii) the occurrence of an incorrect beam deflection angle for the optical path. In contrast to other methods, the reference stiffness method provided a straightforward approach that relied only on a static measurement of the polymer microactuator displacement that could be measured indirectly with a standard silicon cantilever using the AFM. In AFM, an accurate measurement of the stiffness constant is of crucial importance for quantifying the surface force interactions between the probe tip and sample at sub-nanometer resolution (e.g. forces $< 10^{-10}$ Newtons). This ability to measure such small forces with nanometer lateral precision underlies the AFM's unique strength and has significantly impacted on numerous disciplines by quantifying fundamental surface forces (e.g. van der Waals) and biological inter/intra-molecular forces. With the further development of micro and nanoactuators, a similar requirement for quantifying their surface force interactions is envisaged, particularly for chemical sensing and mechanical applications. Thus, as with AFM micron-sized cantilevers, standardized techniques with nanometer sensitivity must be implemented in order to characterize the mechanical properties (e.g. stiffness constant) of similar sized polymer actuators. At present, it is difficult to calculate the stiffness constant of these polymer actuators based on their material properties as they are typically comprised of a composite structure with three different materials. This composite structure makes it very difficult to accurately model the effective elastic modulus due to the complexity of the interrelated individual materials parameters that affect their bulk mechanical properties (e.g. actuation, Young's Modulus, density). Accurate determination of their dimensions, i.e. using optical techniques, can be used to determine the stiffness constant from the Euler-Bernouilli model [10], though may still be limited from non-isotropic properties in the composite structure. Another method is to initially measure the resonant frequency of the microactuators and then calculate the stiffness constant [11]. This again requires a *priori* measurement of the resonant frequency, which may become problematic for polymer microactuators using current detection systems. In general, a major problem has been the complex nature of the polymer actuation mechanisms and lack of analogous classical theories that have hindered the development and conclusive experimental verification of comprehensive 'electro-chemo-mechanical' models of the actuator behaviors. To address these issues, we utilize the highly sensitive optical lever detection system of an AFM, and ability to laterally position a probe with nanometer precision to apply a known load directly at the end of a non-aqueous polymer microactuator. By measuring the resulting displacement, the stiffness constant of the microactuator could easily be determined using approaches based on the reference stiffness calibration method. Importantly, this method was quick and simple, and did not require prior information on the dimensions or elastic modulus of the polymer microactuators.

2. SYNTHESIS OF POLYMER ACTUATORS

The structure and actuation principle of the polymer microactuators used in this paper is illustrated in Fig.1. The laminated structure behaves like a bilayer that generates a simple bending motion. In contrast to a single active polymer layer with uniform strain (i.e. no bending), the inclusion of a middle PVDF layer separating two polymer layers results in differential strain at each layer causing bending , as shown in Fig. 1. The synthesis of this structure starts with the sputter coating of gold particles (a thickness ranging between 10 and 100 °A) on both sides of a PVDF sheet, which is like a filter membrane with a pore size of 0.45 μm and nominal thickness of 110 μm. The coated layers of gold serve to increase the conductivity of the polymer electrodes to be grown. Propylene carbonate (PC, Aldrich), lithium triflouromethanesulfonimide (Li^+TFSI^-, 3M) were used as received. Pyrrole (Merck) was distilled and stored under nitrogen at $-20^{\circ}C$ before use [5, 11]. Using a potentiostat/galvanostat, the polypyrrole layers were grown

galvanostatically on the gold coated PVDF at a current density of 0.1 $mAcm^{-2}$ for 12 hours from the growth solution. Details of other synthesis conditions are reported in [1]. Upon completion of the polymerization, the polymer coated bulk sheet was rinsed with acetone to remove any remaining growth solution and stored in the salt + solvent solution until it was needed for the microfabrication and the AFM measurements.

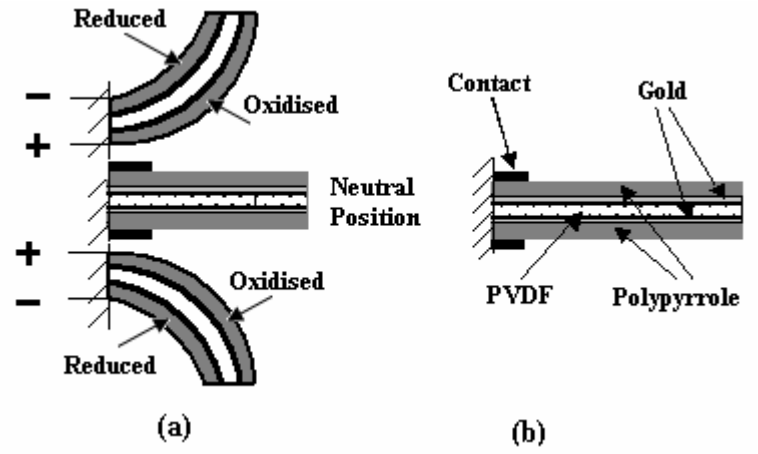

Fig. 1. (a) Schematic representation of the bending principle, and (b) schematic structure of the conducting polymer actuator. This actuator is anion-driven; the anions in the salt move into the positively charged electrode to cause a volume expansion. If it is cation-driven, the cations in the salt move into the negatively charged electrode to cause volume expansion, hence the bending direction will be from the negative electrode to the positive electrode—opposite to what is shown in Fig. 1 (a).

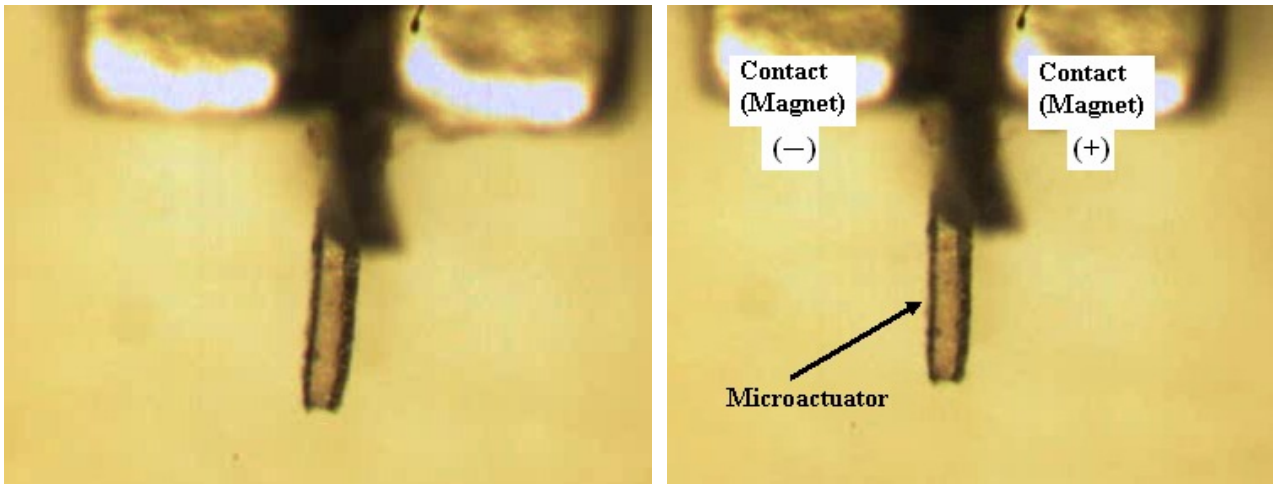

Fig. 2. The optical images of a microactuator under 1V. The images on the right show the neutral positions of the actuators. Two permanent magnets are used to create enough compaction force on two electrically conducting metal plates; in between the microactuator is placed [1].

The structure of the actuator with electrolyte stored in the PVDF membrane functions as an electrochemical cell and is electrically stimulated by applying a potential difference or passing current between the polymer electrodes *via* the contacts. The whole microactuator structure is charged like a capacitor. With the salt ($Li^{+}TFSI^{-}$) used, while the positively charged electrode (the polymer layer) is oxidised, the negatively charged electrode is reduced. To maintain charge neutrality, the negatively charged $TFSI^{-}$ anions move towards the inside of the positively charged polymer electrode and hence cause a volume expansion. While this is happening in the positive electrode/anode, the anions ($TFSI^{-}$) will leave the negatively charged electrode with a volume contraction—opposite volume change. The overall result is that the polymer microactuator will bend towards the negative electrode/cathode, as depicted in Fig. 1a. Volume changes in the polymer occur due to movement of the charge balancing anions in and out of the polymer layers. It is also possible that solvent molecules incorporate into the polymer layers as well due to osmotic effects. The charge transfer between the anode and cathode determines the volume change. The actuation speed and overall volume change also

depends on many electro-chemo-mechanical parameters, including the thickness of the polymer layers, the ion type and sizes, charge injected (potential applied), the ionic concentration, the solvent, and the width of the actuator [5,12]. Optical images of a polymer microactuator activated with an applied potential of 1 V are provided in Fig. 2.

3. ANALYTICAL STIFFNESS MODELS

Because the actuation mechanism of the microactuators is based on the movement of the ions in and out of the polymer layers, the internally induced bending force can be assumed to be analogous to a uniformly distributed load acting on a cantilever beam. The tip deflection of the beam under the uniformly distributed load is [10]

$$y = \frac{F L^3}{24\, EI}\left(8 - 6\lambda + \lambda^3\right), \quad \text{where } \lambda = \frac{L_a}{L} \text{ and } F = L_a\, f_a \tag{1}$$

With reference to Fig.3b, $L_a = L$ *or* $\lambda = 1$ for our microactuators. From Eq.1, the stiffness of the beam is

$$k = 8\frac{EI}{L^3} \tag{2}$$

where $EI = 2b\left(\frac{h_1^3}{3}E_{pvdf} + \frac{h_2^3 - h_1^3}{3}E_{ppy}\right)$, which is the flexural rigidity of the microactuators, and E_{ppy} and E_{pvdf} are the elastic moduli of the PPy and PVDF, respectively. A description of the remaining parameters is provided in Fig.3.

With reference to Eq.2, the stiffness constant is inversely proportional to the cube of the length, and linearly proportional to the actuator width and to the cube of the actuator thickness. This model may look appropriate to calculate the stiffness constant of the cantilevered beams. However, it is unlikely to obtain accurate estimation of the stiffness constant of microactuators. As stated before, the primary reason is that there are a large number of variables and interrelated parameters that affect their actuation, and therefore their modulus of elasticity [13].

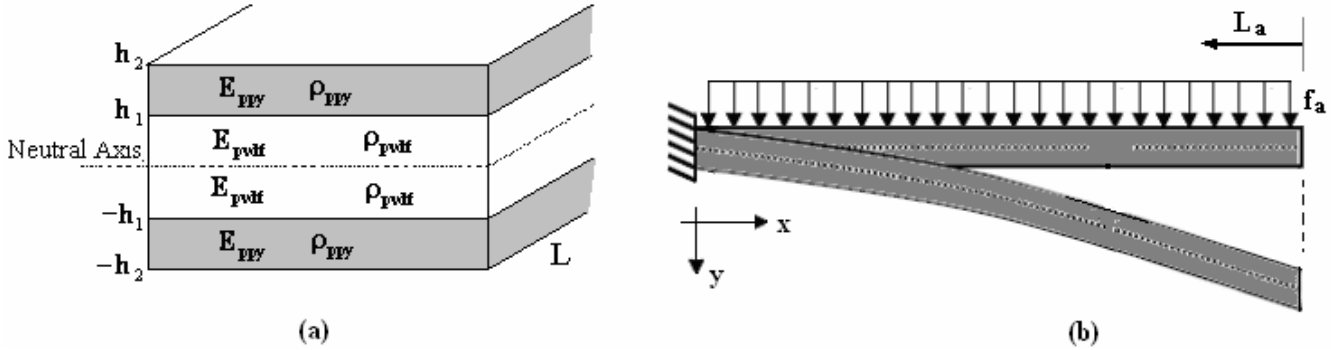

Fig.3. Description of the geometric parameters to formulate the stiffness model of the tri-layer polymer actuators.

In addition to the reference stiffness method used here, the application of another AFM calibration procedure, termed the Sader Method, to determine the polymer microactuator stiffness constant appears feasible. Though this method is yet to be tested on polymer microactuators, this calibration procedure appears promising as it only requires a measurement of the resonant frequency, quality factor and plan view dimensions of the cantilever. Furthermore, it does not require information on the mass or density properties of the actuator materials. This method is valid for cantilever beams with rectangular and non-rectangular cross-sections, where the aspect ratio is > 3 and quality factor greatly exceeds >1 [9]. An alternative method specifically investigated for macro polymer actuators uses a measurement of the resonant frequency to calculate the stiffness constant from the following expression [11], assuming a negligibly small damping constant.

$$\omega_n = \frac{1}{2\pi}\sqrt{\frac{k}{m_e}}, \qquad m_e = \frac{33}{140}m, \quad \Rightarrow k = 9.3056 m\, \omega_n^2 \tag{3}$$

where $m = 2Lbh_1\rho_{pvdf} + 2Lb(h_2 - h_1)\rho_{ppy}$, the first resonant frequency ω_n is in Hertz. This method also necessitates accurate measurements of the actuator dimensions as well as the PPy and PVDF densities (ρ_{ppy}, ρ_{pvdf}) when they are a part of the tri-layer microactuators.

Though these above methods are suitable, we wanted to assess a new approach that circumvented the need to directly measure the displacement (e.g. resonant frequency) of the polymer microactuator. An optical top-down view of the AFM measurement and schematic diagram describing how the stiffness constant is measured are shown in Figs. 4 and 5, respectively. Prior to the stiffness estimation of the microactuator, the stiffness constant of the AFM cantilever, $k_{cantilever}$ used in the experiments was pre-calibrated using the thermal calibration method [8]. For this initial calibration, the inverse lever optical sensitivity (invOLS) was measured for the AFM cantilever by taking a force versus distance curve on a non-compliant surface (i.e. glass slide). The slope of the contact region in these curves represented the invOLS (nm/V) and was used to convert the photodiode voltage cantilever deflection signal into a distance given in meters (typically 10^{-9} m). The AFM cantilever was then positioned directly in the middle and as close to the end of the polymer actuator to avoid errors associated with torsional bending and progressive stiffness changes along its length, respectively. The AFM cantilever was then pushed against the polymer microactuator with a known force, *F,* and the resulting deflection of the AFM cantilever, $D_{cantilever}$ recorded by performing a force versus distance curve. The loading force acting on the polymer microactuator actuator, $F_{actuator}$, resulted in the deflection of the polymer microactuator, $D_{actuator}$, and was equivalent to the applied force of the AFM cantilever, $F_{cantilever}$, where $F_{actuator} = F_{cantilever} = k_{cantilever} \times D_{cantilever}$. During the force measurement, the vertical displacement of the piezo, D_{piezo}, required to move the tip represented the combined deflection of the AFM cantilever tip and polymer microactuator, thus the latter could be given as $D_{actuator} = D_{piezo} - D_{cantilever}$. By knowing $F_{actuator}$ and $D_{actuator}$, simple Hooke's law was used to easily solve for the stiffness constant of the polymer microactuator. This approach is based on the reference stiffness method, which typically pushes an AFM cantilever with known stiffness constant onto an unknown cantilever, though the calculation are nevertheless analogous.

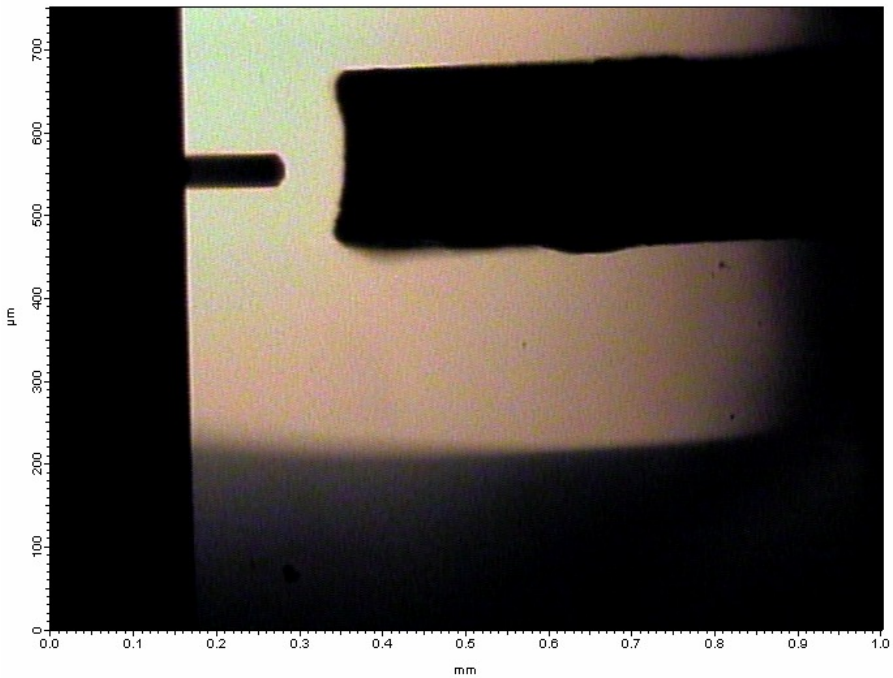

Fig. 4. The microimage of the microactuator with the dimensions of 799 mu x 217 mu x155 mu under the AFM. The silicon AFM cantilever (NSC 15/50, Micromash) has the dimensions of 125 mu x 35 mu x4 mu.

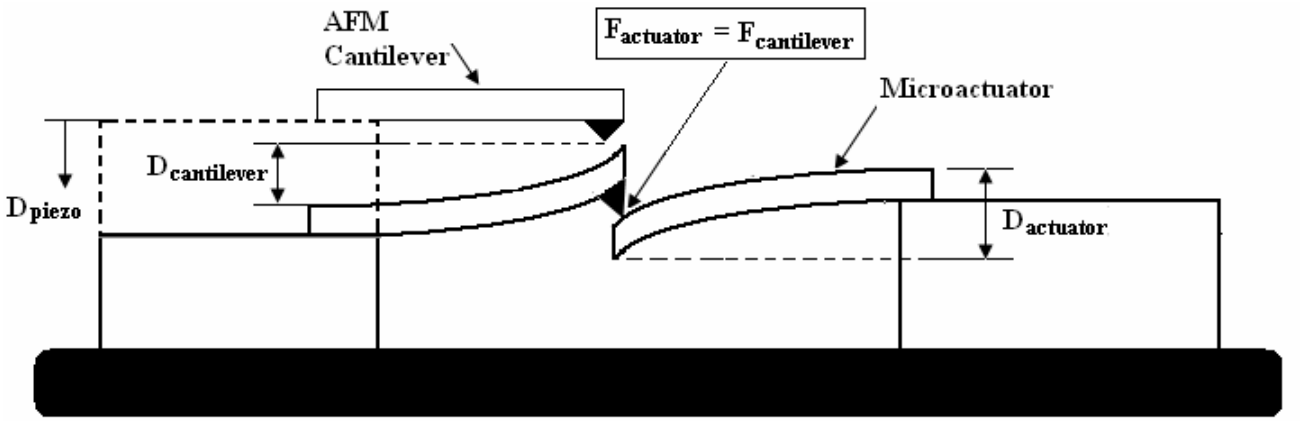

Fig. 5: Schematic representation of the measurement system (not to scale).

4. STIFFNESS MEASUREMENT RESULTS AND DISCUSSION

The stiffness constant of the AFM cantilever used in the measurements was calibrated to be 43 N/m. A polymer microactuator with dimensions of 799 mu x 217 mu x155 mu (length x width x thickness) was used in the measurements and a series of applied forces (100nN, 200nN, 300nN, 400nN, 500nN, 700nN) was applied during the force measurements to assess the effect this parameter on the stiffness constant of the polymer microactuator. The calculated stiffness values for the non-electrically stimulated (passive state) microactuator are presented in Table 1. Two typical measurements are depicted in Fig. 6. At least 10 measurements were taken under each force to evaluate the repeatability of the measurements. . The standard error (SE) of the stiffness values was calculated for each force. It must be noted that the stiffness varies with the contact force. However, the stiffness constants for applied forces ≥ 300 nN show a relatively constant value. These stiffness values can be considered a more accurate representation of the microactuator stiffness in the passive state. This is because a constant compliance is achieved in the force curves (Fig. 6, right curve) that at these higher forces, which is a requirement for accurate determination of the stiffness using the reference spring method outline above. With this in mind, the passive stiffness of the microactuator can be calculated as approximately 18 N/m.

The same microactuator was activated with +500mV input (active state), under which the same AFM force measurements were applied to calculate the active stiffness of the actuator. The stiffness results and the corresponding standard error results are provided in Table 2. The constant stiffness is reached under relatively higher forces ≥ 400 nN. Therefore, the active stiffness of the microactuator considered can be calculated as approximately 22.32 N/m.

The same experiment was repeated under -500mV (active state), where the actuator bent downwards in the opposite direction. Two typical force measurements at different applied loads on the microactuator are depicted in Fig. 7. The stiffness results and the corresponding standard error results are provided in Table 3. Similar to the microactuator activated with +500mV input, the constant stiffness is reached for forces ≥ 400 nN. Therefore, the active stiffness of the microactuator considered can be calculated as approximately 20.2 N/m.

Table 1: Estimated stiffness constants when the microactuator was not activated, i.e. passive.

Applied Force, **F** (nN)	Mean of Stiffness, $\mathbf{k}_{mean}$ (N/m)	Standard Error, SE
100	13.30	0.69
200	16.99	1.27
300	17.79	0.71
400	18.02	1.06
500	17.19	1.50
700	19.22	0.24

There is a small difference observed in the stiffness values between the passive and active states. The increase in stiffness for the active states may be due electrochemical processes occurring in the microactuator manifesting itself as an increase in mechanical energy, though further work is required to validate this given the experimental error in these

reference spring measurements. There was no significant difference in the microactuator stiffness observed between the two active states (i.e. -500mV and +500mV). Further measurements will be conducted on different microactuators, and with the use of different applied potentials, to assess whether synthesis anomalies (e.g. variations in PPy layer thickness) or varying potentials has an influence in the microactuator stiffness.

Table 2: Estimated stiffness constants when the microactuator was activated with +500mV.

Applied Force, **F** (nN)	Mean of Stiffness, $\mathbf{k}_{\mathbf{mean}}$ (N/m)	Standard Error, SE
100	7.89	0.32
200	14.25	0.65
300	17.463	1.12
400	22.87	1.05
500	21.28	1.53
700	22.81	0.87

Table 3: Estimated stiffness constants when the microactuator was activated with -500mV.

Applied Force, **F** (nN)	Mean of Stiffness, $\mathbf{k}_{\mathbf{mean}}$ (N/m)	Standard Error, SE
100	7.85	0.45
200	13.99	0.87
300	18.41	1.17
400	19.96	0.64
500	20.56	1.12
700	20.07	0.87

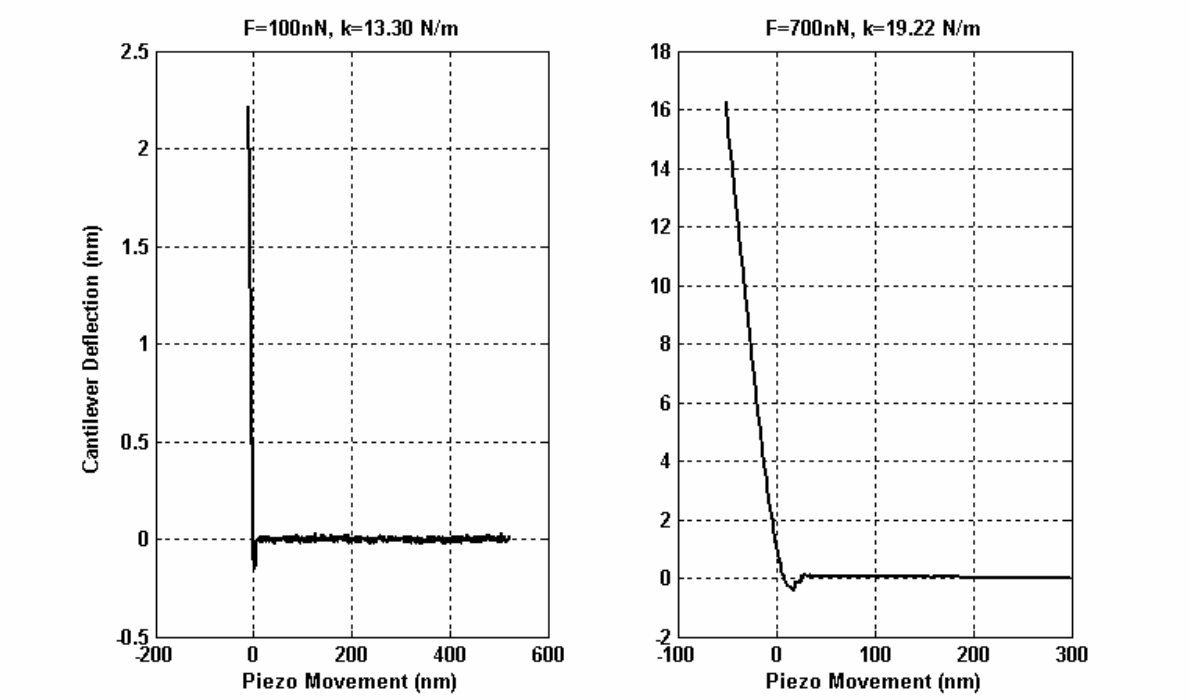

Fig. 6. The right and left plots are recorded under 100 nN and 700 nN, respectively. The actuators were in the passive state.

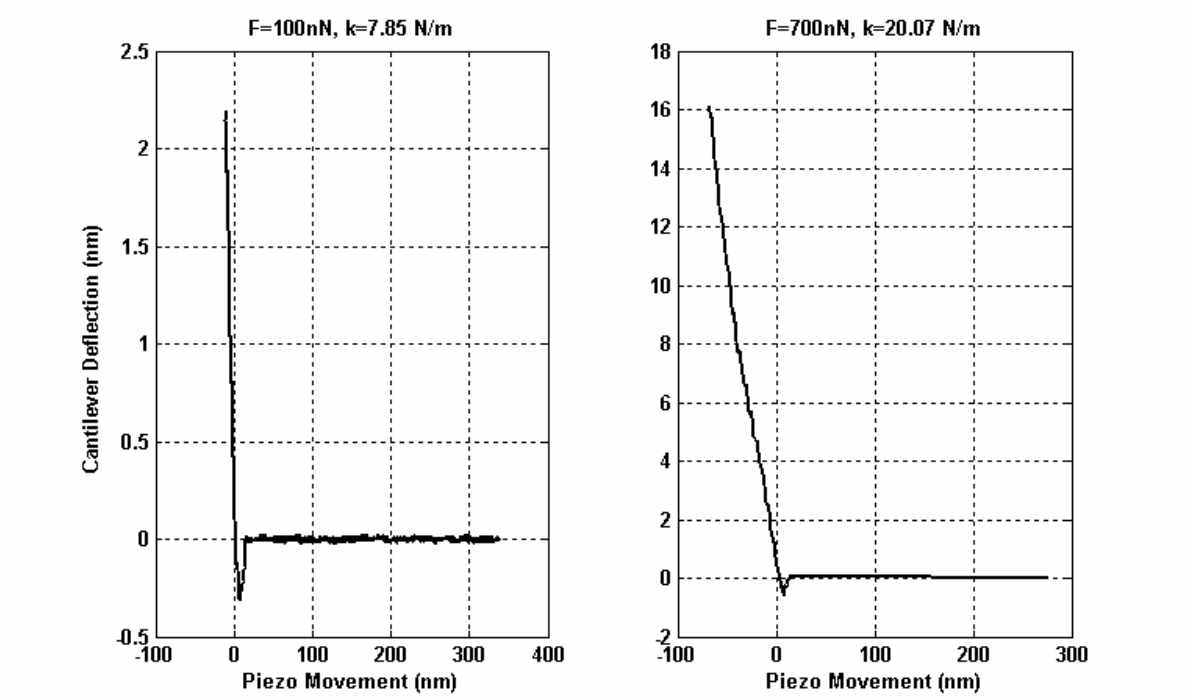

Fig. 7. The right and left plots are recorded under 100 nN and 700 nN, respectively, while -500mV was applied to the microactuator. The tip of the microactuator was bent upward. The AFM cantilever was pushed against the microactuator.

4.1 Error sources

It must be noted that there is an error associated with the stiffness constants calculated from the AFM measurements. The possible sources of the error are associated with the stiffness calibration of the AFM cantilever. This error is on the order of 10 % [8]. Other sources of error may result from penetration or indentation of the PPy layer during the force measurements, the increased wetting of the microactuators as they are electrically activated, and possible dynamic electrochemical changes within the actuator. Further works is underway to analyze the possible influence of these factors.

4.2. Potential applications

The first resonant frequency of the microactuator can be estimated using Eq.3. For the densities $\rho_{ppy} = 1.38 g/cm^3$ and $\rho_{pvdf} = 1.44\ g/cm^3$ [11] the mass of the microactuator is calculated to be 34.163 nanograms. The resulting resonant frequency is determined from Eq. 3, i.e.

$$\omega_n = \sqrt{\frac{k}{9.3056\, m}} \tag{4}$$

For the mean stiffness constants presented in Tables 1-3, the resonant frequencies are calculated to be, 7524.6, 8379.0, and 7971.2 Hertz, respectively.

As one potential application of the microcantilevers is in electrostatic MEMS as an active microswitch, there is a need to know the stiffness of the microcantilevers in order to model and estimate the pull-in voltage (threshold voltage) [14]. The pull-in phenomenon causes instability during the operation of electrostatic MEMS. If the stiffness constant of the microcantilever is known, the pull-in voltage can be considered during the design stage to prevent such instability. The stiffness constant for MEMS switches should be between 5 and 40 N/m, which is encompasses the active passive stiffness of the microactuators. A microswitch based on the microcantilever can find applications in wireless communications and high-isolation switching networks for satellite and radar systems. These switches are alternative to

electrical switches. The reasons are that they have low power consumption, good linearity, and good isolation. One requirement is that the contact between the switch and the surface should not show adhesion problems. The EAP microcantilever or microactuator can overcome this through its built-in actuation without damaging the contact surface. There is no need of intentionally roughening the contact surface to minimize the contact area, and hence prevent adhesion problems.

In other applications such as in the biotechnology as a cell tapper to apply a certain force onto the cell, it is equally important to know the stiffness of the microactuator to calculate the micro and nanoscale forces, like knowing the stiffness constant of an AFM cantilever to measure the nano and piconewton forces.

5. CONCLUSIONS

The stiffness characterization of the conducting polymer based microcantilevers has been performed using measurements provided by an atomic force microscope. The modified reference stiffness method was applied to evaluate the stiffness constants of the microactuators while they were passive and active under a constant potential difference. The uncertainties associated with the stiffness evaluation method are discussed to assess the accuracy of the stiffness values. The experimental results reveal that the method is simple, versatile and easy to implement to determine the stiffness constants of polymer microactuators.

ACKNOWLEDGMENTS

This work was supported in part by a URC Small Grant (2007), ARC Discovery Project (DP0878931), and ARC Centre of Excellence for Electromaterials (CE0561616).

REFERENCES

[1] G. Alici, V. Devaud, P.Renaud, and G. M. Spinks, “Conducting polymer microactuators operating in air”, IOP Journal of Micromechanics and Microengineering, 2008. (Accepted for publication)

[2] G. Alici, and N. N. Huynh, “Performance Quantification of Conducting Polymer Actuators for Real Applications: a Microgripping System”, IEEE/ASME Transactions on Mechatronics, Volume 12, No.1, pp.73 -- 84, February 2007.

[3] G. Alici, G. M. Spinks, N. N. Huynh, L. Sarmadi, and R. Minato, “Establishment of a Biomimetic Device Based on Tri-layer Polymer Actuators – Propulsion Fins”, Journal of Bioinspiration & Biomimetics, Vol.2, No.2, pp. S18-S30, June 2007.

[4] Q. Yao, G. Alici, and G. M. Spinks, “Feedback Control of Tri-layer Polymer Actuators to Improve Their Positioning Ability and Speed of Response”, Sensors and Actuators A, Vol. 144, No.1, pp. 176 – 184, May 2008.

[5] Y. Wu, G. Alici, G.M. Spinks and G.G. Wallace, “Fast tri-layer polypyrrole bending actuators for high speed applications”, Volume: 156, Issues 16-17, Synthetic Metals, pp. 1017-1022, August 1, 2006.

[6] H. J. Butt, B. Cappella, and M. Kappl, “Force measurements with the atomic force microscope: Technique, interpretation and applications”, Surface Science Reports, Vol. 59, pp. 1–152, 2005.

[7] C. A. Clifford, and M. P. Seah, “The determination of atomic force microscope cantilever stiffness constants via dimensional methods for nanomechanical analysis”, Nanotechnology, Vol.16, pp. 1666—1680, 2005.

[8] A. Torii, M. Sasaki, K. Hane, and S. Okuma, “A method for determining the stiffness constant of cantilevers for atomic force microscopy”, Meas. Science Technology, Vol.7, pp. 179 – 184, 1996.

[9] J. E. Sader, J. W. m. Chon, and P. Mulvaney, “Calibration of rectangular atomic force microscope cantilevers”, Review of Scientific Instruments, Vol.70, No.10, pp. 3967 – 3969, 1999.

[10] R.J. Roark and W.C. Young, Formulas for Stress and Strain (New York: McGraw-Hill), 1989.

[11] S. W. John, G. Alici, and C. D. Cook, "Validation of a Resonant Frequency Model for Polypyrrole Trilayer Actuators", IEEE/ASME Transactions on Mechatronics, Vol.13, No.4, pp. 401 – 409, August 2008.

[12] G. Alici, P. Metz, and G. M. Spinks, “A Methodology towards Geometry Optimisation of High Performance Polypyrrole (PPy) Actuators”, Journal of Smart Materials and Structures, Volume 15, pp. 243 – 252, 2006.

[13] G. Alici, B. Mui, and C. Cook, “Bending Modeling and Its Experimental Verification for Conducting Polymer Actuators Dedicated to Manipulation Applications”, Sensors and Actuators A, Volume 126, No.2, pp. 396 – 404, 14 February, 2006.

[14] S. Pamidighantam, R. Puers, K. Baert, and H. A. C. Tilmans, “Pull-in voltage analysis of electrostatically actuated beam structures with fixed-fixed and fixed-free end conditions”, Journal of Micromechanics and Microengineering, Vol.12, pp. 458—464, 2002.